Unconventional thermal effects across first-order magnetic transition in the Ta-doped $HfFe_2$ intermetallic

Pallab Bag, R. Rawat,* and P. Chaddah
UGC-DAE Consortium for Scientific Research, University Campus, Khandwa Road, Indore 452001, India

P. D. Babu and V. Siruguri
UGC-DAE Consortium for Scientific Research, R-5 Shed, Bhabha Atomic Research Centre, Mumbai, India
(Received 29 July 2015; published 12 January 2016)

Unconventional thermal effects across the first-order antiferromagnetic (AFM)-ferromagnetic (FM) transition in an intermetallic alloy are reported. They show instances of warming when heat is extracted from the sample, and cooling when heat is provided to the sample across the AFM-FM transition in Ta-doped $HfFe_2$, thus providing indisputable evidence of metastable supercooled AFM and superheated FM states, respectively. Such thermal effects are observed in a magnetic solid prepared from commercially available materials. The transition proceeds in multiple steps which is interpreted in the framework of quenched disorder broadening of the AFM-FM transition and classical nucleation theory. Measurements in the presence of a magnetic field conform to the above framework.

DOI: 10.1103/PhysRevB.93.014416

I. INTRODUCTION

First-order transitions are characterized by latent heat and transformation from one phase to another phase occurring via nucleation and growth processes. If the heat (ΔQ) extracted from the system is less than its total latent heat (L), then only a fraction ($\propto \Delta Q/L$) of the total system can transform to a low temperature phase. However, this fraction cannot be reduced to an arbitrarily small value as the nuclei below a critical size will be unstable. In the classical nucleation theory, the critical size of the stable nuclei (r^*) is proportional to $(\gamma_{sl} \times T_C)/(\Delta T^* \times \Delta L)$, where γ_{sl} is the interfacial energy, T_C is the equilibrium transition temperature, ΔT^* is the undercooling temperature, and ΔL is the latent heat of the transition of nuclei. Therefore, the transformation from one phase to other phase occurs in a quantum of steps, the size of which is dictated by r^*. With increased undercooling, i.e., with increased metastability of the supercooled state, r^* decreases. The higher the metastability, the smaller is the perturbation required to transform this state into a stable state. For such a transformation during cooling (warming), if the heat removed from (supplied to) the adiabatic system is less than the latent heat of transformation, then the system temperature increases (decreases). Such thermal effects, known as recalescence, are commonly observed during liquid to solid transformations (e.g., water to ice transitions, solid-liquid transitions in NiAl by Kulkarni *et al.* [1], and Al-Nb alloys by Munitz *et al.* [2]). However, observations of similar thermal effects across first-order magnetic transitions in solids are rare. Generally, first-order transitions in solids are broadened due to the presence of quenched disorder. For such materials, there exists a spatial distribution of transition temperatures on the length scale of the correlation length, and for a macroscopic system it leads to a quasicontinuous distribution of transition temperatures, leading to an apparent gradual change in physical properties [3,4], though locally (on the length scale of the correlation length) the transition remains discontinuous [5–7]. To date, there are two examples of magnetic solids with a first-order phase transition where such thermal effects has been reported: ultrahigh purity Er and Dy metals studied by Gschneidner *et al.* [8,9]. Direct observations of such thermal effects were possible due to the ultrahigh purity of the studied system, in addition to the lower heat capacity of the sample as well as the addenda. Here, we show a similar thermal effect around a first-order antiferromagnetic (AFM)-ferromagnetic(FM) transition in a transition metal alloy (Ta-doped $HfFe_2$) prepared from commercial grade (purity $\approx$ 99.99%) constituent elements. Quenched disorder broadening results in a multiple step transition, which is further verified by measurements in the presence of a magnetic field.

The hexagonal parent $HfFe_2$ compound is ferromagnetic at room temperature, which becomes antiferromagnetic with $>$14% Ta substitution for Hf [10,11]. For $\approx$ 14%–22% Ta substitution, a first-order AFM to FM transition with $\approx$1% volume expansion has been reported [10–12]. The first-order transition in these systems has been of interest due to the observation of large magnetocaloric effects [13] and the recent observation of kinetic arrest [14,15]. The composition studied in the present work, namely, $Hf_{0.82}Ta_{0.18}Fe_2$, shows a first-order AFM-FM transition around 220 K.

II. EXPERIMENTAL DETAILS

The sample is prepared using commercially available Ta and Fe of purity 99.99% and Hf of purity 99.9% (exclusive of 2% Zr). Constituent elements were weighed in their atomic ratio and arc-melted three to four times under an inert argon gas atmosphere. A Rietveld analysis of a powder x-ray diffraction (XRD) pattern of the as-prepared sample is found to be consistent with a hexagonal lattice with a space group $P6_3/mmc$, and it showed that the sample is single phase with lattice parameters $a = 4.9292$ Å and $c = 8.0636$ Å [14]. Magnetization measurements were carried out

*rrawat@csr.res.in

using Quantum Design superconducting quantum interference device-vibrating sample magnetometer (SQUID-VSM) and Physical Property Measurement System (PPMS) vibrating sample magnetometer (VSM). The heat capacity was measured using a home-made heat capacity setup based on the semiadiabatic heat pulse method [16,17] along with a 8-T superconducting magnet system from Oxford Instruments, U.K.

III. RESULTS AND DISCUSSION

The results of magnetization (M) and heat capacity (C_P) measured across first-order AFM-FM transition temperatures are shown in Figs. 1(a) and 1(b), respectively. Magnetization data, which are collected during cooling and subsequent warming in the presence of a 0.1 T magnetic field, show an AFM-FM transition around 215.5 and 219.5 K, respectively. In the AFM state, isothermal application of a magnetic field can induce an AFM to FM transition; a typical curve is shown in the inset of Fig. 1(a) at 250 K. It shows an increase of about 1.4 μ_B/f.u. around 4 T with a narrow hysteresis for increasing and decreasing field cycles. The heat capacity, which is measured during warming, exhibits a sharp peak

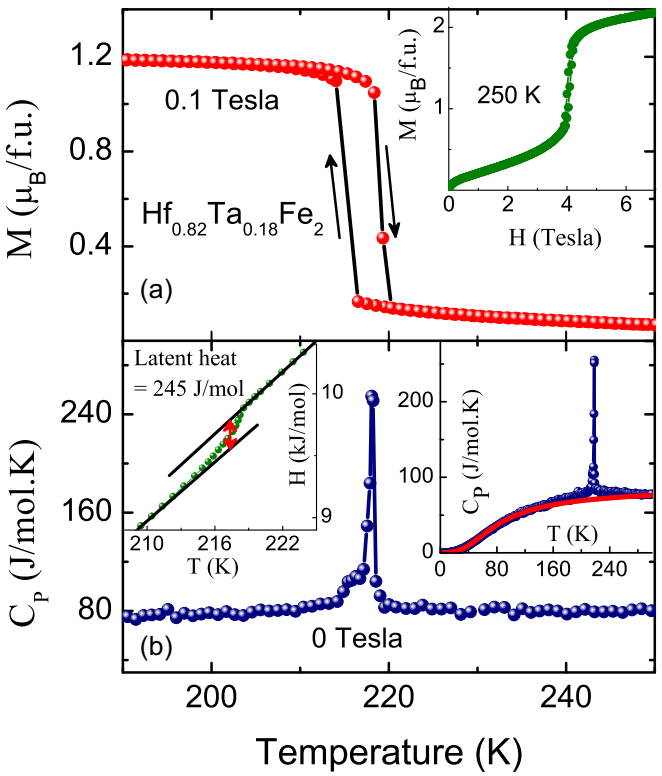

FIG. 1. (a) Magnetization measured in the presence of 0.1 T during cooling and subsequent warming in $Hf_{0.82}Ta_{0.18}Fe_2$. The inset shows the field-induced AFM-FM transition with an isothermal application of a magnetic field at 250 K. (b) Heat capacity measured during warming in the absence of an applied magnetic field across a first-order AFM-FM transition. The left inset shows the enthalpy variation across the first-order transition and the right inset shows the measured heat capacity along with the sum of the linear term with a coefficient of 24 mJ/mol K^2 and a Debye term with a Debye temperature of 355 K.

around 218 K, as highlighted in the main panel of Fig. 1(b). The right inset shows the measured heat capacity (in blue circles) along with the sum (red triangles) of linear (with a coefficient 24 mJ/mol K^2) and Debye contributions (with a Debye temperature 355 K). The estimate of the latent heat of the transition is done from the enthalpy curve calculated from the measured heat capacity, as shown in the inset of Fig. 1(b). The enthalpy curve below and above the transition region is fitted with a linear equation and extrapolated to the transition temperature. The difference between these two curves at the transition temperature gives the latent heat of the transition, which is found to be 245 J/mol. These values (entropy change, latent heat, Debye temperature, etc.) are in close agreement with those reported by Wada *et al.* [18].

Figure 2 shows some typical sample temperature versus time curves during cooling and warming across the AFM-FM transition temperature. These curves were collected using the same setup as used for measuring heat capacity [16,17]. For these measurements the sample holder heater is switched off and heat flow to or from the sample is controlled by varying the radiation shield temperature (or surrounding temperature) at a constant rate. As shown in the top panel of Fig. 2, during cooling, multiple instances of temperature rise are observed when heat is extracted from the sample around the transition region. The rise in sample temperature when heat is extracted from the sample provides unambiguous evidence of the transformation of a metastable supercooled AFM state into a stable FM state. The temperature jumps are found to be as large as 340 mK [Fig. 2(a), jump No. 3]. With an increasing ramp rate, these thermal effects shift to a lower temperature and the step size reduces. Rapid cooling allows a deeper supercooling (and hence transformation at a lower temperature) which, in the case of metallic glasses, is used to avoid crystallization. The step is expected to vanish if the heat extracted from the system becomes equal to or larger than the released latent heat. Similar temperature versus time scans, taken during warming, are shown in the bottom panel of Fig. 2. In this case, for the lowest heating rate [Fig. 2(d)], the sample temperature decreases [though with a much smaller magnitude, as highlighted in the inset of Fig. 2(d)] within the temperature region of the first-order transition. This observation of cooling when heat is supplied to the system is evidence of the transformation from a superheated FM state to a stable AFM state. However, the net changes in sample temperature were found to be much smaller (at the most 50 mK) when compared to those observed during cooling (about 340 mK). For higher ramping rates, these features diminish. This is more akin to a water to ice transition, where superheating is found to be absent as melting starts from the surface. Similar to the ice to water transition, in the present system, too, the FM to AFM transition is also accompanied with a decrease in unit cell volume. The asymmetry in transformation during cooling and heating has been a feature of many magnetoelastic AFM-FM transitions; for example, in the case of FeRh, the AFM-FM transformation is shown to be asymmetric under certain conditions and explained due to the difference in nucleation and growth mechanisms for an AFM to FM and back transformation [19,20]. For the present sample also, the M-T measurement [see Fig. 1(a)] indicates a broader AFM-FM transition during warming when compared to cooling.

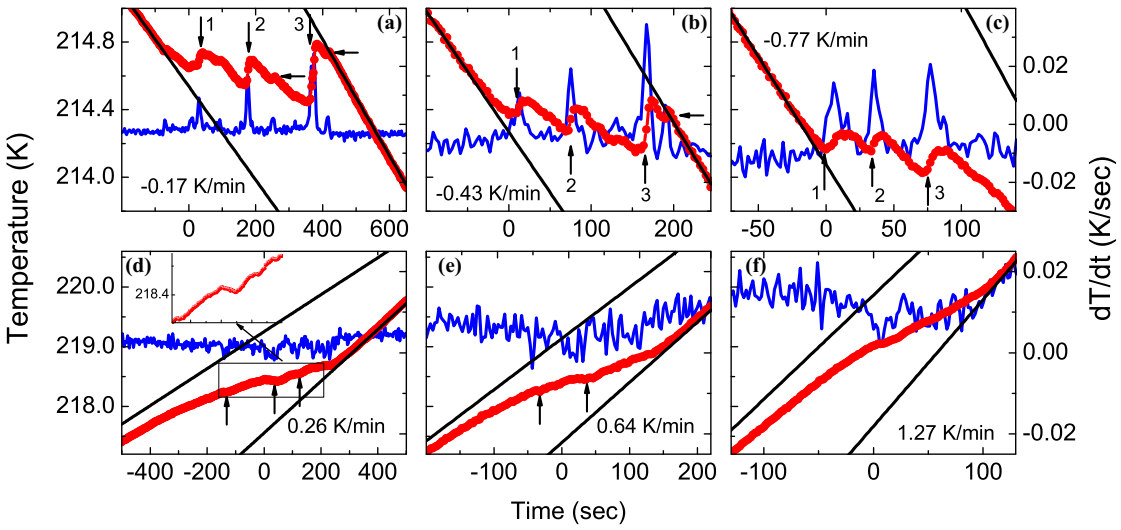

FIG. 2. Time dependence of the sample temperature (right axis) and its derivative (left axis) across a first-order AFM-FM transition in $Hf_{0.82}Ta_{0.18}Fe_2$ during cooling (top panel) and warming (bottom panel) for various temperature ramp rates in the absence of an applied magnetic field. Vertical arrows highlight instances of an increase in sample temperature when heat is extracted from the sample and a decrease in sample temperature while heat is supplied to the sample. Horizontal arrows mark the instances when a jump occurs at a higher temperature than the start temperature of the preceding jump.

Multiple step jumps across a field-induced first-order transition in isothermal magnetization have been observed in a variety of systems at low temperatures [21,22]. In the case of the $Hf_{1-x}Ta_xFe_2$ system, too, the compositions around $x = 0.23$ show a steplike increase in isothermal magnetization across a field-induced AFM to FM transition [14]. These magnetization jumps are found to diminish with an increase in temperature. These studies also showed that the kinetic arrest dominates at low temperatures (below around 35 K) for these compositions $x \approx 0.23$. In such a case the heat released due to the field-induced transformation of one region triggers the transformation in the other region, resulting in a cascade of transitions with field [22], whereas, in the present case, the sample temperature increases when heat is extracted from the sample and it is observed in the absence of magnetic field [Fig. 2(a)] or at a constant applied magnetic field [Figs. 3(a)–3(c)].

The multiple jumps can be interpreted in terms of a broad first-order transition due to quenched disorder, where each instance of a jump indicates a transformation of a different region of the sample. The latent heat associated with these jumps is listed in Table I and is found to be as high as 49 J/mol for the 340 mK jump [jump No. 3 of Fig. 2(a)]. A comparison with the total latent heat of the transition suggests that feature No. 3 in the cooling curve corresponds to about 20% of the sample and the sum of all jumps accounts for about 44% of the sample.

It is worth mentioning here that multiple jumps in the temperature versus time curve in the case of ultrahigh purity Er have been taken as an indication of the transformation through unknown intermediate states [9]. However, direct evidence of such intermediate states is yet to be found. In light of the present investigation, the multiple step transition for the Er sample can be explained considering disorder broadening. Their heat capacity data of Dy and Er systems also support this interpretation since in the case of Er, a small but nonzero width of the transition is evident in the temperature dependence of the heat capacity, whereas for Dy, which showed a singular behavior in heat capacity (i.e., no broadening), a single step transition is observed.

The contention that the observed multiple steps are a consequence of quenched disorder broadening is further tested by studying these thermal effects in the presence of a magnetic field. With the application of a magnetic field, the transition temperature T_C increases and, therefore, the critical size of the nuclei is expected to increase. In addition, the transition becomes broader and, therefore, the temperature difference between consecutive instances of an inverse temperature rise is expected to increase. Some typical cooling temperature versus time and heat capacity curves in the presence of a 1–4 T magnetic field are shown in Figs. 3(a)–3(e). As the applied magnetic field increases, the transition temperature is shifted to a higher temperature and the spacing between two consecutive jumps increases. The number and magnitude of temperature jumps decrease with magnetic field, and at 4 T, no such thermal effects are observed. As the T_C increases, the critical size of the nuclei (r^*) increases and this decreased surface to volume ratio results in a smaller heat release during recalescence. These thermal effects are further suppressed due to the decreased latent heat of transition with increasing magnetic field, as shown in the inset of Fig. 3(e). The maximum value of the magnetocaloric effect calculated from the heat capacity is found to be $-\Delta S_{th}$(isothermal change in entropy) $= 1.3 \pm 0.2$ J/mol K, and ΔT_{ad}(adiabatic change in temperature) $= 3.8 \pm 0.5$ K for a magnetic field change of 0–4 T. The ΔS_{th} values are comparable with the existing literature [13]. The adiabatic change in temperature (ΔT_{ad}) is significantly smaller than the shift in transition temperature (T_C) with magnetic field (e.g., it is about 27 K for a magnetic field change from 0 to 4 T). It could be due to the significant lattice contribution to heat capacity or a large increase in lattice entropy with an increase in temperature in this temperature range.

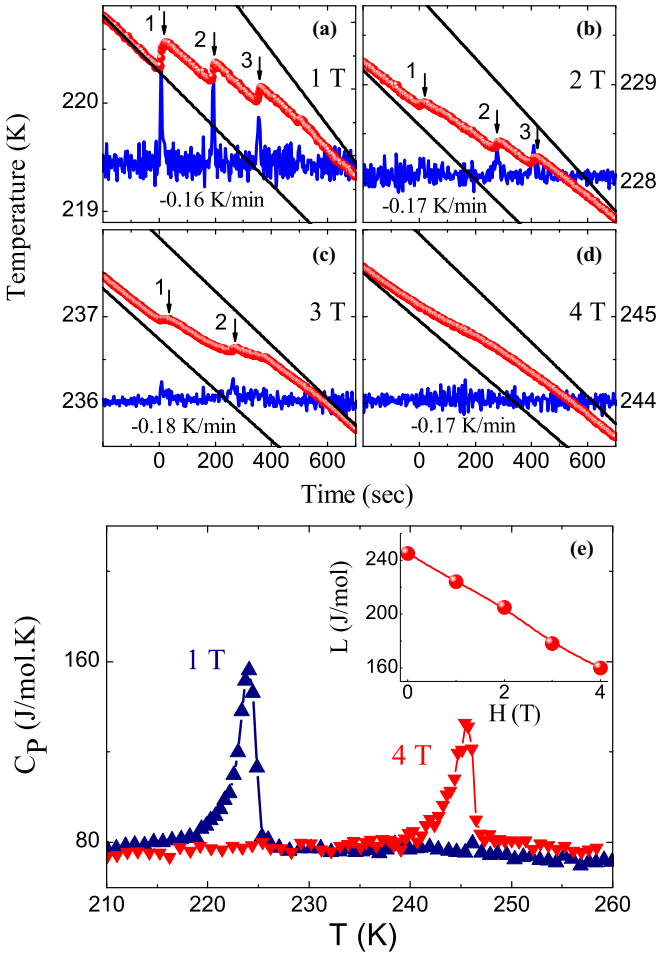

FIG. 3. (a)–(d) Time dependence of the sample temperature across a first-order AFM to FM transition in $Hf_{0.82}Ta_{0.18}Fe_2$ during cooling for 1, 2, 3, and 4 T. The instances of a temperature rise (indicated by vertical arrows) while heat is extract from the sample vanish with increasing magnetic field. The blue line curves show the derivative of respective curves on a scale of −0.015 to +0.045 K/s. (e) Heat capacity measured during warming in the presence of 1 and 4 T magnetic fields. The inset shows the variation of latent heat with increasing magnetic field.

Another unconventional feature in the temperature versus time curves shown in Fig. 2(a) is that the start temperature of some of the subsequent jumps is not necessarily lower than the start temperature of a preceding jump. Such instances are marked by horizontal arrows in Figs. 2(a) and 2(b). For a disordered broadened first-order transition due to quenched disorder, the region with the higher supercooling limit will be transformed first during cooling. In this picture, a jump at a higher temperature than the preceding one seems to indicate that regions with a lower supercooling limit are transforming first. It is possible that the FM region nucleated in the preceding step acts as a nucleation center for the subsequent step, resulting in a FM transformation at a higher temperature. In the case of $La_{0.5}Ca_{0.5}MnO_3$, a dramatic increase in resistivity with thermal cycling below the transition temperature T_C has been explained due to the presence of an AFM phase obtained during the previous cooling, which results in an enhancement of the low temperature phase during subsequent warming up to T_C [23].

TABLE I. Temperature rise (ΔT in K) and associated latent heat (ΔL in J/mol) for jumps labeled in Figs. 2 and 3.

	Jump No.		
	1	2	3
Magnetic field (T)/ramp rate (K/min)	$\Delta T/\Delta L$	$\Delta T/\Delta L$	$\Delta T/\Delta L$
0/0.2	0.15/26	0.28/33	0.34/48
0/0.4	0.08/32	0.14/33	0.31/49
0/0.8	0.09/32	0.09/33	0.13/49
1/0.2	0.24/33	0.17/23	0.13/20
2/0.2	0.03/32	0.06/16	0.06/12
3/0.2	0.02/18	0.03/16	

IV. CONCLUSIONS

To conclude, unconventional thermal effects associated with the transformation of metastable supercooled/superheated to stable states have been observed. This transformation results in warming (cooling) when heat is extracted from (supplied to) the system. This is an observation in a bulk magnetic solid prepared with commercial grade purity materials, thereby showing a broad first-order transition. The transformation takes place in multiple steps, which is interpreted as a distribution of transformation temperatures over the sample volume as a result of quenched disorder. These features are qualitatively explained in the framework of classical nucleation theory which is tested further with measurements in the presence of a magnetic field. Incidentally, there is a striking similarity between the AFM-FM transition in the present system and the water to ice transition, e.g., supercooling but no superheating and a higher volume of the low temperature state as compared to the high temperature state, etc. If this analogy holds true, then the nucleation of the AFM phase is expected to be on the surface or grain boundary.

ACKNOWLEDGMENT

R. J. Choudhary, UGC-DAE Consortium for Scientific Research Indore, is acknowledged for magnetization measurements.

[1] N. S. Kulkarni and K. T. Hong, Metall. Mater. Trans. A **29**, 2221 (1998).
[2] A. Munitz, A. B. Gokhlae, and R. Abbaschian, J. Mater. Sci. **35**, 2263 (2000).
[3] Y. Imry and M. Wortis, Phys. Rev. B **19**, 3580 (1979).
[4] P. Chaddah, arXiv:1405.1162.
[5] R. Rawat, P. Kushwaha, D. K. Mishra, and V. G. Sathe, Phys. Rev. B **87**, 064412 (2013).

[6] S. B. Roy, G. K. Perkins, M. K. Chattopadhyay, A. K. Nigam, K. J. S. Sokhey, P. Chaddah, A. D. Caplin, and L. F. Cohen, Phys. Rev. Lett. **92**, 147203 (2004).
[7] A. Soibel, E. Zeldov, M. Rappaport, Y. Myasoedov, T. Tamegai, S. Ooi, M. Konczykowski, and V. B. Geshkenbeink, Nature (London) **406**, 282 (2000).
[8] V. K. Pecharsky, J. K. A. Gschneidner, and D. Fort, Scr. Mater. **35**, 843 (1996).
[9] K. A. Gschneidner, V. K. Pecharsky, and D. Fort, Phys. Rev. Lett. **78**, 4281 (1997).
[10] Y. Nishihara and Y. Yamaguchi, J. Phys. Soc. Jpn. **51**, 1333 (1982).
[11] Y. Nishihara and Y. Yamaguchi, J. Phys. Soc. Jpn. **52**, 3630 (1983).
[12] P. Bag, S. Singh, P. D. Babu, V. Siruguri, and R. Rawat, Physica B **448**, 50 (2014).
[13] J. F. Herbst, C. D. Fuerst, and R. D. McMichael, J. Appl. Phys. **79**, 5998 (1996); S. Huang, D. Wang, Z. Han, Z. Su, S. Tang, and Y. Du, J. Alloys Compd. **394**, 80 (2005); Z. Han, D. Wang, S. Huang, Z. Su, S. Tang, and Y. Du, *ibid.* **377**, 75 (2004); L. V. B. Diop, J. Kastil, O. Isnard, Z. Arnold, and J. Kamarad, *ibid.* **627**, 446 (2015).
[14] R. Rawat, P. Chaddah, P. Bag, P. D. Babu, and V. Siruguri, J. Phys.: Condens. Matter **25**, 066011 (2013).
[15] V. R. Reddy, R. Rawat, A. Gupta, P. Bag, V. Siruguri, and P. Chaddah, J. Phys.: Condens. Matter **25**, 316005 (2013).
[16] R. Rawat and I. Das, Phys. Rev. B **64**, 052407 (2001).
[17] P. Bag, V. Singh, and R. Rawat, Rev. Sci. Instrum. **86**, 056102 (2015).
[18] H. Wada, N. Shimamura, and M. Shiga, Phys. Rev. B **48**, 10221 (1993).
[19] S. Maat, J.-U. Thiele, and E. E. Fullerton, Phys. Rev. B **72**, 214432 (2005).
[20] C. Baldasseroni, C. Bordel, C. Antonakos, A. Scholl, K. H. Stone, J. B. Kortright, and F. Hellman, J. Phys.: Condens. Matter **27**, 256001 (2015).
[21] D. L. Strandburg, S. Legvold, and F. H. Spedding, Phys. Rev. **127**, 2046 (1962); H. Weitzel and J. Hirte, Phys. Rev. B **37**, 5414 (1988); G. C. DeFotis, B. Lee, H. A. King, and J. Hammann, J. Magn. Magn. Mater. **177–181**, 173 (1998); C. M. Wynn, M. A. Girtu, J. S. Miller, and A. J. Epstein, Phys. Rev. B **56**, 14050 (1997); R. Mahendiran, A. Maignan, S. Hebert, C. Martin, M. Hervieu, B. Raveau, J. F. Mitchell, and P. Schiffer, Phys. Rev. Lett. **89**, 286602 (2002); E. M. Levin, K. A. Gschneidner, Jr., and V. K. Pecharsky, Phys. Rev. B **65**, 214427 (2002); A. Haldar, K. G. Suresh, and A. K. Nigam, J. Phys.: Conf. Ser. **200**, 032021 (2010).
[22] Y. Mudryk, V. K. Pecharsky, and K. A. Gschneidner, Jr., in *Handbook of Physics and Chemistry of Rare Earth*s, edited by J.-C. G. Bünzli and V. K. Pecharsky (North-Holland, Amsterdam, 2014), Vol. 44, p. 283.
[23] P. Chaddah, K. Kumar, and A. Banerjee, Phys. Rev. B **77**, 100402 (2008).